

## Two dimensional model of pulsatile flow of a dusty fluid through a tube with axisymmetric constriction \*

Anju Saini<sup>1†</sup>, V.K. Katiyar<sup>2</sup>, M. Parida<sup>3</sup>

<sup>1</sup> Centre for Transportation Systems, Indian Institute of Technology Roorkee, Roorkee-247667, India

<sup>2</sup> Department of Mathematics, Associate Faculty in Centre for Transportation Systems, Indian Institute of Technology Roorkee, Roorkee-247667, India

<sup>3</sup> Department of Civil Engineering, Associate Faculty in Centre for Transportation Systems, Indian Institute of Technology Roorkee, Roorkee-247667, India

(Received September 04 2015, Accepted December 18, 2015)

**Abstract.** The purpose of this paper is to conduct a comprehensive investigation of the two-dimensional natural convection flow of a dusty fluid. Thus, the incompressible boundary layer flow of a two-phase particulate suspension is explored numerically over a tube with axisymmetric constriction. The work is concerned to study the pulsatile flow behavior of particulate suspensions through a tube with sinusoidal wall vibrations. Finite difference method has been used to solve the unsteady nonlinear Navier-Stokes equations in cylindrical coordinate system assuming axial symmetry under laminar flow condition so that the problem efficiently turns into two-dimensional form. An extensive quantitative study is performed through numerical computations of the preferred quantities having physiological importance through their graphical demonstration so as to authenticate the applicability of the current model. Results for velocity of fluid and dust particles and wall shear stress distribution have been discussed.

**Keywords:** pulsatile flow, particulate suspensions, finite difference method, wall shear stress

### 1 Introduction

In the procedure by which raindrops are produced by the coalescence of tiny droplet which might be considered as solid particles, these areas consist of fluidization, environmental pollution, due to investigative the solid particles progress previous to coalescence, combustion and more lately, blood flow<sup>[14]</sup>. Study of pulsatile blood flow in the cardiovascular system because of its importance in the latest history has influenced scientific thinking. Blood has been treated either as two fluids consisting of a boundary layer of pure plasma close to the wall or as a single homogeneous combination covering the properties of a Newtonian fluid and in the blood vessel somewhere else the complete blood, according to a number of the papers<sup>[17]</sup>. However after using these two models, several important outcomes have been achieved, no approximation of the errors has been occurred in the estimation<sup>[1, 23, 24]</sup>.

Saffman<sup>[22]</sup> is a pioneer in giving simple analytical model for motion of dusty fluid with large number of dust particles suspended in it. Many fluid dynamists have tried to solve the problems of dusty fluid flow through circular and cylindrical pipes and in between parallel plates etc., under some boundary conditions. Barron<sup>[6]</sup> has tried to study magneto fluid dynamic flow in Frenet frame field system for the duration of the next part of 20th century. Bagewadi and Gireesha<sup>[4]</sup>; Bagewadi and Shantharajappa<sup>[5]</sup>; Gireesha et al.<sup>[13]</sup>; Rashmi et al.<sup>[3]</sup> has extended the study to plasma flow, electrodynamic flow and dusty gas flow in Frenet frame field system.

\* Financial support by grant in aid to one of the authors (Dr. Anju Saini), from National Board for Higher Mathematics (NBHM), Department of Atomic Energy, Government of India is gratefully acknowledged.

† E-mail address: anju.iitr@gmail.com.

In petroleum industry and in the refinement of crude oil, the influence of dust particles in viscous flows has large significance. Erosion of dirt by natural winds and dust entrainment in a cloud through nuclear detonation are further main applications of dust particles in boundary layer<sup>[28]</sup>. Moreover fluidization, flow in rocket tubes, combustion, paint spraying and in recent times blood flows in capillaries happen in a broad series of regions of technological significance. Already enough effort has been finished on models of dusty fluid flow. Authors like Amos<sup>[2]</sup>; Datta and Dalal<sup>[9]</sup>; Datta and Mishra<sup>[10]</sup>; Saini et al.<sup>[25]</sup> have studied the fluid flow due to pulsatile pressure gradient. Further, due to a much lengthy annular pipe Dalal et al.<sup>[8]</sup>; Datta and Dalal<sup>[9]</sup>; Datta and Mishra<sup>[10]</sup> have studied the pulsatile flow and heat transfer of a dusty fluid. Gupta and Gupta<sup>[14]</sup>; Ramamurthy and Rao<sup>[20]</sup> studied under time dependent pressure gradient. Nabil et al.<sup>[12]</sup> studied the effect of couple stresses on pulsatile hydro magnetic poiseuille flow. A more recent analysis of convective dusty flow past a vertical stretching sheet with internal heat absorption was given by Nandkeolyar and Sibanda<sup>[19]</sup>. They also reduced the boundary layer equations into a set of similar equations and solved them by *bvp4c* routine of Matlab. Further, Anwar Bg et al.<sup>[7]</sup> conducted a numerical study of single and two phase models in a circular tube and reported that single-phase and two-phase models yield the same results for fluid flow but different results for thermal fields. Another study regarding single and two-phase models of nanofluid heat transfer in wavy channel was done by Rashidi et al.<sup>[21]</sup> and investigated the behavior of heat transfer coefficient, temperature and velocity distributions. Siddiqua et al.<sup>[26]</sup> and Dey<sup>[11]</sup> has studied dusty fluid flow and periodic pressure gradient in a rotating channel.

The present work is concerned with the pulsating flow of a fluid with dusty particles in a pipe consisting of axisymmetric distributed constrictions described by the wall radius  $R$ . A two dimensional plane of the pipe is considered. Through an extra drag force caused by dust particles the fluid flow is assumed to be governed by Navier-Stokes equations. Governing equations are solved numerically by using suitable finite difference method. The expressions for the velocities of fluid and dust particles and wall shear stress have been obtained.

## 2 Model formulation

### 2.1 Mathematical model

Consider the laminar flow of an incompressible fluid that contains small solid particles, whose number density ( $N_0$ ) (constant) is large enough to define average properties of the dust particles at a point through a symmetrical constricted two-dimensional tube with sinusoidal wall vibrations, whose boundary (Fig. 1) is specified by

$$R = R_0 + \alpha_0 \sin \frac{2\pi}{\lambda} z, \quad (1)$$

where  $\alpha_0$  is the wave amplitude,  $\lambda$  is the wavelength,  $z$  is the longitudinal axis of the pipe and  $R_0$  is the pipe width.

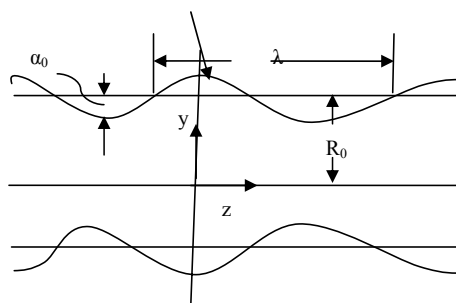


Fig. 1: Geometry of channel with sinusoidal wall variation

Under these assumptions, the equations governing the fluid flow containing solid particles may be written in the cylindrical coordinates system as equation of continuity:

$$\eta = R_0 + \alpha_0 \sin \frac{2\pi}{\lambda} z,$$

$$\frac{\partial u_r}{\partial r} + \frac{u_r}{r} + \frac{\partial u_z}{\partial z} = 0, \quad (2)$$

$$\frac{\partial v_r}{\partial r} + \frac{v_r}{r} + \frac{\partial v_z}{\partial z} = 0. \quad (3)$$

Equation of axial momentum

$$\frac{\partial u_z}{\partial t} + u_r \frac{\partial u_z}{\partial r} + u_z \frac{\partial u_z}{\partial z} = -\frac{1}{\rho} \frac{\partial p}{\partial z} + \nu \left( \frac{\partial^2 u_z}{\partial r^2} + \frac{1}{r} \frac{\partial u_z}{\partial r} + \frac{\partial^2 u_z}{\partial z^2} \right) + \frac{KN_0}{\rho} (v_z - u_z), \quad (4)$$

$$\frac{\partial v_z}{\partial t} + v_z \frac{\partial v_z}{\partial z} + v_r \frac{\partial v_z}{\partial r} = \frac{K}{m} (u_z - v_z). \quad (5)$$

Equation of radial momentum

$$\frac{\partial u_r}{\partial t} + u_r \frac{\partial u_r}{\partial r} + u_z \frac{\partial u_r}{\partial z} = -\frac{1}{\rho} \frac{\partial p}{\partial r} + \nu \left( \frac{\partial^2 u_r}{\partial r^2} + \frac{1}{r} \frac{\partial u_r}{\partial r} + \frac{\partial^2 u_r}{\partial z^2} - \frac{u_r}{r^2} \right) + \frac{KN_0}{\rho} (v_r - u_r), \quad (6)$$

$$\frac{\partial v_r}{\partial t} + v_z \frac{\partial v_r}{\partial z} + v_r \frac{\partial v_r}{\partial r} = \frac{K}{m} (u_r - v_r). \quad (7)$$

Here  $u_z(r, z, t)$  and  $u_r(r, z, t)$  represent the axial and the radial velocity components of the fluid respectively,  $v_z(r, z, t)$  and  $v_r(r, z, t)$  represents the axial and the radial velocity components of the dust particles respectively,  $p$  is the static pressure,  $N_0$  is the number density and  $m$  is the mass of the dust particle. Since the lumen radius  $R$  is sufficiently smaller than the wavelength  $\lambda$  of the pressure wave, Eqs. (6) and (7) simply reduce to  $\frac{\partial p}{\partial r} = 0$  and thus can be omitted. The pressure gradient  $\partial p / \partial z$  appearing in Eq. (4), is given by

$$-\frac{\partial p}{\partial z} = A_0 + A_1 \cos \omega, \quad t > 0$$

and  $K = 6\pi\mu r_p$ , where  $A_0$  =constant amplitude of the pressure gradient,  $A_1$  =amplitude of the pulsatile component giving rise to systolic and diastolic pressure.

$$\omega = 2\pi f_p,$$

where  $f_p$  is the pulse frequency and  $r_p$  radius of the dust particle.

## 2.2 Boundary conditions

All at rest position of the system, the flow is zero.

$$u_r = 0, \quad v_r = 0, \quad u_z = 0, \quad v_z = 0.$$

There is no radial flow along the axis of the artery and the axial velocity gradient of the streaming blood may be assumed to be equal to zero.

$$u_r = 0, \quad \frac{\partial u_z}{\partial r} = 0, \quad v_r = 0, \quad \frac{\partial v_z}{\partial r} = 0.$$

At the surface of the wall,

$$u_r = 0, \quad v_r = 0, \quad u_z = 0, \quad v_z = 0.$$

i.e., the no-slip boundary condition is imposed.

### 3 Non-dimensionalisation of the problem

#### 3.1 Transformation of the governing equations

Using the following non-dimensional quantities

$$u_x = \frac{u_r}{u_0}, \quad u_y = \frac{u_z}{u_0}, \quad v_x = \frac{v_r}{u_0}, \quad v_y = \frac{v_z}{u_0}, \quad x = \frac{r}{R}, \quad y = \frac{z}{R},$$

$$p = \frac{p'}{\rho u_0^2}, \quad \tau = \frac{t u_0}{R}, \quad Re = \frac{R u_0}{\nu}, \quad B = \frac{K R N_0}{\rho}, \quad \gamma = \frac{m u_0}{K R}.$$

Eqs. (2) to (5) together with boundary conditions take the following form:

$$\frac{\partial u_x}{\partial x} + \frac{u_x}{x} + \frac{\partial u_y}{\partial y} = 0, \quad (8)$$

$$\frac{\partial u_y}{\partial \tau} + u_x \frac{\partial u_y}{\partial x} + u_y \frac{\partial u_y}{\partial y} = -\frac{\partial p}{\partial y} + \frac{1}{Re} \left( \frac{\partial^2 u_y}{\partial x^2} + \frac{1}{x} \frac{\partial u_y}{\partial x} + \frac{\partial^2 u_y}{\partial y^2} \right) + B(v_y - u_y), \quad (9)$$

$$\frac{\partial v_x}{\partial x} + \frac{v_x}{x} + \frac{\partial v_y}{\partial y} = 0, \quad (10)$$

$$\frac{\partial v_y}{\partial \tau} + v_x \frac{\partial v_y}{\partial x} + v_y \frac{\partial v_y}{\partial y} = \frac{u_y - v_y}{\gamma}. \quad (11)$$

#### 3.2 Transformation of the boundary conditions

$$\begin{array}{lll} u_x = 0, & v_x = 0, u_y = 0, & v_y = 0, \text{ at } \tau = 0. \\ u_x = 0, & \frac{\partial u_y}{\partial x} = 0, v_x = 0, & \frac{\partial v_y}{\partial x} = 0, \text{ at } x = 0. \\ u_x = 0, & v_x = 0, u_y = 0, & v_y = 0, \text{ at } x = 1. \end{array}$$

The Finite difference scheme is used to solve the governing transformed equation by using central difference approximations for all the spatial derivatives<sup>[27]</sup>. The iterative method has been found to be quite effective in solving the equation numerically for different time periods. The time step was chosen to be  $\Delta t = 0.001$ ,  $\Delta y = 0.05$  and  $\Delta x = 0.05$  is the grid spacing. These results are subsequently used to solve equations numerically.

To use finite difference scheme Eqs. (8), (9) and (10) (at  $x = 0$ ), converts as

$$\begin{aligned} \lim_{x \rightarrow 0} \frac{u_x}{x} &= \lim_{x \rightarrow 0} \frac{\partial u_x}{\partial x}, \\ \lim_{x \rightarrow 0} \frac{1}{x} \frac{u_y}{x} &= \lim_{x \rightarrow 0} \frac{\partial^2 u_y}{\partial x^2}, \\ \lim_{x \rightarrow 0} \frac{v_x}{x} &= \lim_{x \rightarrow 0} \frac{\partial v_x}{\partial x}. \end{aligned}$$

### 4 Discretization of the component

The discretization of axial velocity  $u_z(x, y, t)$  is written as  $u_z(x_i, y_i, t_k)$  or  $(u_z)_{ij}^k$ . We define

$$\begin{aligned} x_i &= i \cdot \Delta x; \quad i = 1, 2, \dots, N, \quad \text{where } x_N = 1.0 \\ y_j &= j \cdot \Delta y; \quad j = 1, 2, \dots, M, \\ t_k &= (k - 1) \cdot \Delta; \quad k = 1, 2, \dots. \end{aligned}$$

Using the discretization techniques the axial velocity from Eq. (9) (at  $x = 0$ ), has its discretized form as:

$$\begin{aligned}(u_y)_{i,j}^{k+1} = & (u_y)_{i,j}^k \left[ 1 - \frac{4.\Delta\tau}{\Delta x^2} \cdot \frac{1}{Re} - \frac{2.\Delta\tau}{\Delta y^2} \cdot \frac{1}{Re} - B.\Delta\tau \right] - \frac{\Delta\tau}{2.\Delta x} \left[ (u_x)_{i,j}^k \cdot (u_y)_{i+1,j}^k + (u_x)_{i,j}^k \cdot (u_y)_{i-1,j}^k \right] \\ & - \frac{\Delta\tau}{2.\Delta y} \left[ (u_y)_{i,j}^k \cdot (u_y)_{i,j+1}^k + (u_y)_{i,j}^k \cdot (u_y)_{i,j-1}^k \right] + \frac{2.\Delta\tau}{Re.(\Delta x)^2} \left[ (u_y)_{i+1,j}^k + (u_y)_{i-1,j}^k \right] \\ & + \frac{\Delta\tau}{Re.(\Delta y)^2} \left[ (u_y)_{i,j+1}^k + (u_y)_{i,j-1}^k \right] + B.\Delta\tau \cdot (v_y)_{i,j}^k + (A_0 + A_1 \cos(\omega\tau R/u_0)) \Delta\tau,\end{aligned}$$

at  $0 < x \leq 1$ , the Eq. (9) becomes

$$\begin{aligned}(u_y)_{i,j}^{k+1} = & (u_y)_{i,j}^k \left[ 1 - \frac{2.\Delta\tau}{(\Delta x)^2} \cdot \frac{1}{Re} - \frac{2.\Delta\tau}{(\Delta y)^2} \cdot \frac{1}{Re} - B.\Delta\tau \right] - \frac{\Delta\tau}{2.\Delta x} \left[ (u_x)_{i,j}^k \cdot (u_y)_{i+1,j}^k + (u_x)_{i,j}^k \cdot (u_y)_{i-1,j}^k \right] \\ & - \frac{\Delta\tau}{2.\Delta y} \left[ (u_y)_{i,j}^k \cdot (u_y)_{i,j+1}^k + (u_y)_{i,j}^k \cdot (u_y)_{i,j-1}^k \right] + \frac{\Delta\tau}{Re.(\Delta y)^2} \left[ (u_y)_{i,j+1}^k + (u_y)_{i,j-1}^k \right] \\ & + (u_y)_{i+1,j}^k \left[ \frac{\Delta\tau}{Re.x.2.\Delta x} + \frac{\Delta\tau}{Re.(\Delta x)^2} \right] + (u_y)_{i-1,j}^k \left[ \frac{\Delta\tau}{Re.(\Delta x)^2} - \frac{\Delta\tau}{Re.x.2.\Delta x} \right] \\ & + B.\Delta\tau \cdot (v_y)_{i,j}^k + (A_0 + A_1 \cos(\omega\tau R/u_0)) \Delta\tau.\end{aligned}$$

After discretization, the radial velocity can be calculated from the Eq. (8) (at  $x = 0$ )

$$(u_x)_{i+1,j}^{k+1} = (u_x)_{i,j}^{k+1} - \frac{\Delta x}{2.\Delta y} \left[ (u_y)_{i,j+1}^{k+1} - (u_y)_{i,j}^{k+1} \right]$$

at  $0 < x \leq 1$ , the Eq. (8) becomes

$$(u_x)_{i+1,j}^{k+1} = \left( 1 - \frac{\Delta x}{x} \right) (u_x)_{i,j}^{k+1} - \frac{\Delta x}{\Delta y} \left[ (u_y)_{i,j+1}^{k+1} - (u_y)_{i,j}^{k+1} \right].$$

The axial velocity of dust particles can be observed from the Eq. (11) and its discretized form is

$$\begin{aligned}(v_y)_{i,j}^{k+1} = & \left( 1 - \frac{\Delta\tau}{\gamma} \right) (v_y)_{i,j}^k + \frac{\Delta\tau}{\gamma} (u_y)_{i,j}^k - \frac{\Delta\tau}{2.\Delta x} \cdot (v_x)_{i,j}^k \left[ (v_y)_{i+1,j}^k - (v_y)_{i-1,j}^k \right] \\ & - \frac{\Delta\tau}{2.\Delta y} \cdot (v_y)_{i,j}^k \left[ (v_y)_{i,j+1}^k - (v_y)_{i,j-1}^k \right].\end{aligned}$$

The radial velocity of dust particles can be calculated from the Eq. (10) (at  $x = 0$ ), with its discretized form as

$$(v_x)_{i+1,j}^{k+1} = (v_x)_{i,j}^{k+1} - \frac{\Delta x}{2.\Delta y} \cdot \left[ (v_y)_{i,j+1}^{k+1} - (v_y)_{i,j}^{k+1} \right],$$

at  $0 < x \leq 1$ , the Eq. (10) becomes

$$(v_x)_{i+1,j}^{k+1} = \left( 1 - \frac{\Delta x}{x} \right) \cdot (v_x)_{i,j}^{k+1} - \frac{\Delta x}{\Delta y} \cdot \left[ (v_y)_{i,j+1}^{k+1} - (v_y)_{i,j}^{k+1} \right],$$

The initial and boundary conditions in discretized form are as follows:

$$\begin{aligned}(u_x)_{1,j}^k = 0, & \quad (u_y)_{0,j}^k = (u_y)_{2,j}^k, & \quad (v_x)_{1,j}^k = 0, & \quad (v_y)_{0,j}^k = (v_y)_{2,j}^k, \\ (u_x)_{N+1,j}^k = 0, & \quad (u_y)_{N+1,j}^k = 0, & \quad (v_x)_{N+1,j}^k = 0, & \quad (v_y)_{N+1,j}^k = 0, \\ (u_x)_{i,j}^1 = 0, & \quad (u_y)_{i,j}^1 = 0, & \quad (v_x)_{i,j}^1 = 0, & \quad (v_y)_{i,j}^1 = 0.\end{aligned}$$

At last the wall share stress is defined as

$$\tau_w = \mu \left( \frac{\partial u_z}{\partial r} + \frac{\partial u_r}{\partial z} \right), \tag{12}$$

or  $\tau_w = \mu \cdot \frac{u_0}{R} \left( \frac{\partial u_y}{\partial x} + \frac{\partial u_x}{\partial y} \right).$

In the discretized form Eq. (12) can be written as

$$(\tau_w)_i^k = \mu \cdot \frac{u_0}{R} \left[ \frac{(u_y)_{i+1,j}^k - (u_y)_{i-1,j}^k}{2\Delta x} + \frac{(u_x)_{i,j+1}^k - (u_x)_{i,j-1}^k}{2\Delta y} \right]. \tag{13}$$

### 5 Results and discussion

Numerical computations have been carried out using the following parameter values [15, 16, 18].

$$R_0 = 0.37 \text{ cm}, \quad N_0 = 0.02504 \times 10^6 / \text{cm}^3, \quad u_0 = 0.3 \text{ cm/s}, \quad r_p = 50 \text{ nm}, \quad m = 0.0002 \text{ gm},$$

$$\mu = 0.039 \text{ g/cm.s}, \quad \rho = 1.06 \text{ g/cm}^3, \quad f_p = 1.2 \text{ Hz}, \quad A_0 = 10 \text{ gm/cm}^2 \text{ s}^2, \quad A_1 = 0.2A_0, \quad \omega = 8$$

For different time periods Fig. 2 explains the variation of the axial velocity profile of fluid at  $z = 20 \text{ mm}$ .

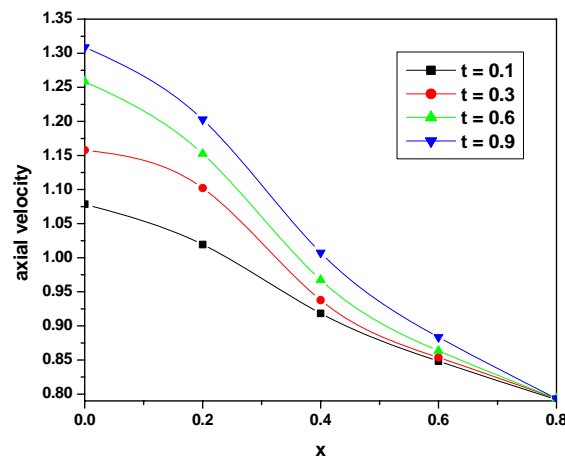


Fig. 2: Axial velocity profile of fluid for different time at  $z = 20 \text{ mm}$

The pumping action of heart created the pulsatile pressure gradient which is directly responsible for the flow profiles. The curve shifted beyond the origin when the time increases from 0.1 sec to 0.3 sec. Again due to the diastole, the axial velocity increases at  $t = 0.6 \text{ sec}$ . Obviously, the streaming blood is much higher than the non-Newtonian values. It is due to the fact that it has a high shear rate flow, which increases the axial velocity profile, if flowing blood is treated as Newtonian. Thus the axial velocity profile is affected by the non-Newtonian characteristics of the flowing blood.

Fig. 3 shows the radial velocity profile of fluid at  $z = 20 \text{ mm}$ . The radial velocity component is varying radially for different time period. It is found to be increasing from zero on the axis with positive values as one move away from it. At last it reaches some finite value on the wall surface.

For different time periods Fig. 4 explains the variation of the axial velocity profile of particles at  $z = 20 \text{ mm}$ . The axial velocity increases as time increases from  $t = 0.1$  to  $0.9$ . But at  $t = 0.1$  and  $t = 0.3$  the velocity become constant throughout after that at  $t = 0.6$  and  $t = 0.9$  the velocity decreases continuously.

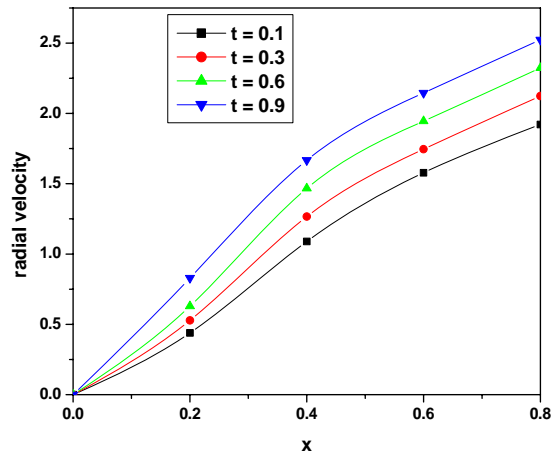


Fig. 3: Radial velocity profile of fluid for different time at  $z = 20$  mm

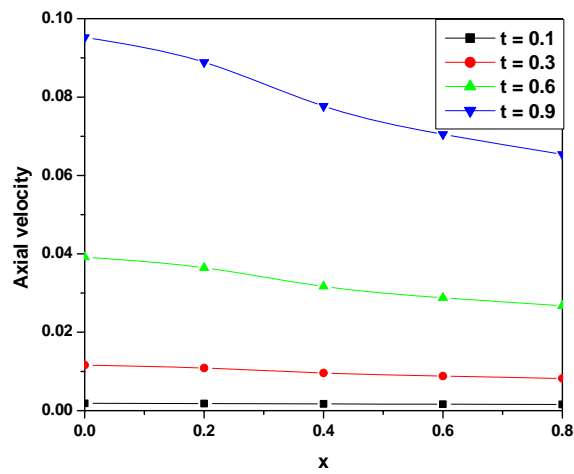


Fig. 4: Axial velocity profile of particles for different time at  $z = 20$  mm

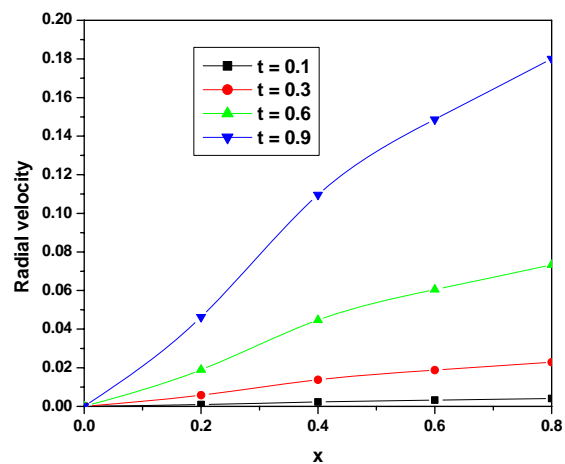


Fig. 5: Radial velocity profile of particles for different time at  $z = 20$  mm

For different time periods Fig. 5 explains the variation of the radial velocity profile of particles at  $z = 20$  mm. It is found to be increasing from zero on the axis with positive values. At last it reaches some finite value on the wall surface.

In Figs. 2 to 5, we have plotted the velocity profiles for the fluid and dust particles for different time periods. From these figures it is observed that the fluid and dust particles possess a maximum velocity on the axis of the tube and fluid particles move faster than the dust particles.

At last Fig. 6 shows the non-Newtonian rheology of the flowing blood and the variation of wall shear stress for various values of the amplitude of the wave  $\alpha_0$ . For all cases the wall shear stress is pulsatile in nature. The flow separation decreases by increasing the value of  $\alpha_0$ .

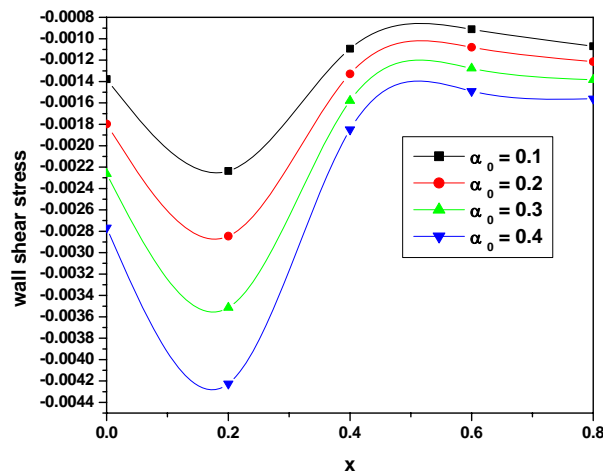


Fig. 6: Variation of the wall shear stress for different  $\alpha_0$  at  $z = 20$  mm and  $t = 0.3$  sec

The wall shear stress in an extremely small approach in comparison to the amplitude of the wave is affected by the non-Newtonian rheology of the blood.

## 6 Conclusion

In the present investigation, two-phase dusty boundary layer flow for two-dimensional case is analyzed over a symmetrical constricted tube. Numerical results for two dimensional pulsatile blood flows in stenotic arteries and to study the effect of the non-Newtonian viscosity of blood on the flow behavior have been presented by this analysis. The results show that as the degree of the stenosis area severity enhance, the blood pressure increases extremely drastically in the upstream region of the stenotic artery. It is also shown that the velocity profile of the blood flow and the magnitude of the wall shear stresses have important effects by the non-Newtonian performance of blood.

## References

- [1] N. Ahmed, J. K. Goswami, D. P. Barua. MHD transient flow with hall current past an accelerated horizontal porous plate in a rotating system. *Open Journal of Fluid Dynamics*, 2013, **3**(04): 278.
- [2] E. Amos, A. Ogulu. Magnetic effect on pulsatile flow in a constricted axis-symmetric tube. *Indian Journal of Pure and Applied Mathematics*, 2003, **34**(9): 1315–1326.
- [3] C. Bagewadi. Unsteady flow of a dusty fluid between two oscillating plates under varying constant pressure gradient. *Novi Sad Journal of Mathematics*, 2007, **37**(2): 25–34.
- [4] C. Bagewadi, B. Gireesha. A study of two dimensional unsteady dusty fluid flow under varying temperature. *International Journal of Applied Mechanics and Engineering*, 2004, **9**(4): 647–653.



- [5] C. Bagewadi, A. Shantharajappa. A study of unsteady dusty gas flow in frenet frame field. *Indian Journal of Pure and Applied Mathematics*, 2000, **31**(11): 1405–1420.
- [6] R. M. Barron. Steady plane flow of a viscous dusty fluid with parallel velocity fields. *Tensor NS*, 1977, **31**(1): 271–274.
- [7] O. A. Béq, M. Rashidi, M. Akbari, A. Hosseini. Comparative numerical study of single-phase and two-phase models for bio-nanofluid transport phenomena. *Journal of Mechanics in Medicine and Biology*, 2014, **14**(01): 1450011.
- [8] D. Dalal, N. Datta, S. Mukherjea. Unsteady natural convection of a dusty fluid in an infinite rectangular channel. *International Journal of heat and mass transfer*, 1998, **41**(3): 547–562.
- [9] N. Datta, D. Dalal. Pulsatile flow and heat transfer of a dusty fluid through an infinitely long annular pipe. *International Journal of Multiphase Flow*, 1995, **21**(3): 515–528.
- [10] N. Datta, S. K. Mishra. Unsteady couette flow and heat transfer in a dusty gas. *International Communications in Heat and Mass Transfer*, 1983, **10**(2): 153–162.
- [11] D. Dey. Hydro-magnetic oscillatory dusty fluid flow with volume fraction and periodic pressure gradient in a rotating channel. *International Journal Research in Applied Science & Engineering Technology*, 2015, **3**: 869–877.
- [12] N. T. El-Dabe, S. M. El-Mohandis. Effect of couple stresses on pulsatile hydromagnetic poiseuille flow. *Fluid Dynamics Research*, 1995, **15**(5): 313.
- [13] B. Gireesha, C. Bagewadi, B. Prasannakumara. Flow of unsteady dusty fluid under varying pulsatile pressure gradient in anholonomic co-ordinate system. *Electronic Journal of Theoretical Physics*, 2007, **4**(14): 9–16.
- [14] R. Gupta, S. Gupta. Flow of a dusty gas through a channel with arbitrary time varying pressure gradient. *Zeitschrift Für Angewandte Mathematik UND Physik ZAMP*, 1976, **27**(1): 119–125.
- [15] Z. Ismail, I. Abdullah, N. Mustapha, N. Amin. A power-law model of blood flow through a tapered overlapping stenosed artery. *Applied Mathematics and Computation*, 2008, **195**(2): 669–680.
- [16] J. N. Kapur. *Mathematical models in Biology and Medicine*. Affiliated East-West Press, 1985.
- [17] D. Liepsch, A. Seemann, J. Siekmann. Note on wave propagation in a thin elastic tube containing a viscous fluid. *Journal of Biomechanics*, 1985, **18**(9): 685–694.
- [18] P. K. Mandal. An unsteady analysis of non-newtonian blood flow through tapered arteries with a stenosis. *International Journal of Non-Linear Mechanics*, 2005, **40**(1): 151–164.
- [19] R. Nandkeolyar, P. Sibanda. On convective dusty flow past a vertical stretching sheet with internal heat absorption. *Journal of Applied Mathematics*, 2013, **2013**.
- [20] V. Ramamurthy, U. Rao. The steady streaming generated by a vibrating plate parallel to a fixed plate in a dusty fluid. *Fluid Dynamics Research*, 1987, **2**(1): 47.
- [21] M. M. Rashidi, A. Hosseini, I. Pop, S. Kumar, N. Freidoonimehr. Comparative numerical study of single and two-phase models of nanofluid heat transfer in wavy channel. *Applied Mathematics and Mechanics*, 2014, **35**(7): 831–848.
- [22] P. Saffman. On the stability of laminar flow of a dusty gas. *Journal of Fluid Mechanics*, 1962, **13**(01): 120–128.
- [23] A. Saini, V. Katiyar, Pratibha. Effects of first-order chemical reactions on the dispersion coefficient associated with laminar flow through the lungs. *International Journal of Biomathematics*, 2014, **7**(02): 1450021.
- [24] A. Saini, V. Katiyar, Pratibha. Numerical simulation of gas flow through a biofilter in lung tissues. *World Journal of Modeling and Simulation*, 2015, **11**(1): 33–42.
- [25] A. Saini, V. Katiyar, Pratibha, Devdatta. Effects of first-order chemical reactions on the dispersion coefficient associated with laminar flow through the lungs. *Journal of Applied Mathematics and Mechanics*, 2010, **6**(15): 46–57.
- [26] S. Siddiq, M. A. Hossain, S. C. Saha. Two-phase natural convection flow of a dusty fluid. *International Journal of Numerical Methods for Heat & Fluid Flow*, 2015, **25**(7): 1542–1556.
- [27] G. D. Smith. *Numerical solution of partial differential equations: finite difference methods*. Oxford University Press, 1985.
- [28] C. Vishalakshi, B. P. Kumara, et al. Transition motion of a magneto dusty fluid between a non-torsional oscillating plate and a long wavy wall. *International Journal of Mathematical Archive*, 2012, **3**(10).

